Journal of ELECTRONIC MATERIALS, Vol. 44, No. 9, 2015
DOI: 10.1007/s11664-015-3742-4

Analysis of Defects on Chemically-Treated CdZnTe Surfaces

A. HOSSAIN,[1,3] A.E. BOLOTNIKOV,[1] G.S. CAMARDA,[1] Y. CUI,[1] R. GUL,[1] K.-H. KIM,[2] U.N. ROY,[1] X. TONG,[1] G. YANG,[1] and R.B. JAMES[1]

1.—Brookhaven National Laboratory, Upton, NY 11973, USA. 2.—Department of Radiologic Science, Korea University, Seoul 136-703, Korea. 3.—e-mail: hossain@bnl.gov

In this work, we focused on investigating the various defects that extend into the near-surface region of CdZnTe (CZT) crystals, and on exploring processing techniques for producing a smooth, non-conductive surface that is ideal for growing thin films and depositing contacts. We determined the surface's features and the chemical species present using atomic-force microscopy, x-ray photoelectron spectroscopy, and scanning electron microscopy (SEM), coupled with energy-dispersive spectroscopy. We revealed crystallographic defects, e.g., sub-grains and dislocations on the CZT crystals' surfaces, after employing selected chemical etchants, and then characterized them using optical microscopy, SEM and optical profilometer. Our experimental data imply that the surface defects and chemical species induced by chemical processing may alter the material's interfacial behavior, and ultimately significantly influence the performance of radiation detectors.

Key words: CdZnTe, substrate and radiation detector, dislocations, chemo-mechanical polishing, metal–semiconductor interface

INTRODUCTION

Cadmium zinc telluride (CdZnTe/CZT) is the leading semiconductor material used for X- and gamma-ray detectors operating at room temperature.[1,2] In addition, it is often used as a substrate material for infra-red active/passive sensor devices due to its lattice-match with mercury-cadmium-telluride epilayers.[3,4] Although CZT crystals are in advanced stages of development, and the popularity of their deployment in different fields of application is growing quickly, some problems related to their bulk and surface properties still remain which adversely influence the crystals' charge-transport properties, and can degrade the overall performance of devices fabricated from these crystals.[5,6]

Sub-grains and dislocations are among the common defects observed in presently available commercial-grade CZT crystals; they are primarily generated during the crystal growth and post-growth annealing processes. These defects are usually not traceable by conventional IR microscopy, which often misleads the vendors about the consistency of the quality and performance. Reports indicate that dislocations laid in the sub-grain boundaries accumulate impurities, secondary phases, and Te inclusions that trap charge-carriers and alter the local distributions of the electric field.[7] Besides these bulk defects, the crystals' surfaces also play a critical role in influencing the device's performance. An imperfect surface creates a source of charge trapping that enhances the surface leakage current; in some cases, it causes an accumulation of charge that becomes the source of device polarization. Furthermore, mechanical and chemical processing creates undesirable features and species at the surface can alter the properties of the fabricated devices.

In this work, we explored dislocation-related defects in CZT crystals that extend into the surface or the near-surface region by employing selected chemical etchants. We also studied the surface and interface states after processing the crystals via mechanical and chemo-mechanical polishing to produce an ideal, smooth, non-conductive surface for growing thin films and depositing metal

(Received January 28, 2015; accepted March 9, 2015; published online March 28, 2015)

contacts. We determined the surface's features and chemical species by atomic force microscopy (AFM), x-ray photoelectron spectroscopy (XPS), and scanning electron-microscopy (SEM), coupled with energy-dispersive spectroscopy (EDS).

EXPERIMENTAL PROCEDURES

We deployed four CZT samples in two sets. Two samples ($10 \times 10 \times 5$ mm^3) in set-1 were used for investigating extended defects in the bulk by revealing the features on the (111)A and (111)B oriented surfaces using selective chemical etchants. The other two samples in set-2 were used for determining the surface features and their electrical properties; therefore, we selected detector-grade crystals with a high resistivity (5×10^{10} Ω-cm) and a high mobility-lifetime product ($\mu\tau_e = 3.5 \times 10^{-3}$ cm^2/V) rather than using orientated samples. All the samples were mechanically polished, first using SiC abrasive papers, and then with a fine-grade alumina powder. Afterwards, the samples were chemo-mechanically polished (CMP) with a multi-tex soft pad moistened with a solution of 2% bromine-methanol and ethylene glycol, and were then thoroughly cleaned in a multi-step process to remove any residual Br from the surfaces.

We etched one sample from set-1 for 1 min with an aqueous solution of hydrofluoric acid, nitric acid, and silver nitrate, and then blow-dried it in pressurized nitrogen gas. The etched surfaces were investigated and imaged under an optical microscope. We also captured the 3D profile of one of the etched samples from set-1 using an optical profilometer.

We registered the AFM images of the set-2 samples before and after CMP to determine the surface roughness. Afterwards, we carried out an XPS experiment to observe the formation of new chemical species. We deposited 2000-Å Au on one surface for one of the set-2 samples using the e-beam evaporator method and annealed it at below 100°C for 20 min. We scanned the Au-CZT interface under scanning electron microscopy (SEM), coupled with energy-dispersive spectroscopy (EDS). Finally, we determined the diffusion profile of the Au into CZT in an XPS experiment by gradually etching off the Au by argon sputtering, which was integrated into the XPS system.

RESULTS AND DISCUSSION

Extended Defects

Sub-grain boundaries and dislocations are the critical bulk defects usually found in most commercial CZT crystals, regardless of the techniques by which they were grown. The optical images of their surfaces in Fig. 1 show examples of such defects in the annealed THM-grown crystals, as revealed by chemical etching. Figure 1a reveals the dislocation etch-pits on one surface, mainly decorating the sub-grain boundaries. These defects are often spread throughout the bulk as linear and cellular networks at different crystallographic orientations[8] and emerging on to the crystals' surfaces. They act as short-circuit channels, as well as trapping centers that hinder the normal transport of charge carriers, while inducing unexpected noise in the devices. Figure 1b displays some Te-rich secondary-phase defects randomly distributed throughout the crystal's surface. Such features are observed only in post-growth annealed samples. Our experimental data show that such hexagonal defects are generated by the reactions of Cd atoms with Te inclusions during annealing in a Cd overpressure at temperatures above the melting point of Te. These features are three-dimensional ones, and, in most cases, the core is empty, as in the example shown in Fig. 2. We believe that this is due to the impact of interactions between the Te inclusions (depending on their size) and the Cd atoms under temperature and pressure that generate empty cores and stresses around them. We detailed these features in our previous report.[8] Such defects in the CZT crystals' surface are problematic when growing films for a detector or an imaging device. They also are detrimental for depositing metal contacts for a gamma-ray radiation detector; eventually, they degrade the device's performance.

Surface Processing

A smooth, non-conductive ideal crystal/substrate surface is a prerequisite for growing thin films and depositing contacts for producing high-quality devices, because an imperfect surface creates a source of charge trapping that enhances the surface-leakage current. In our previous work,[9] we reported on the effects of various chemical etchants used to process the crystals' surfaces on the performance of detectors. In this study, we experimentally determined the CZT crystals' surface roughness before and after chemical treatment, and the effects of treatment on the surface resistivity and carrier concentration. We also observed the diffusion profile of deposited gold on the CMP surface at the metal–semiconductor interface.

Figure 3 shows the AFM images of surface roughness of polished- and chemically polished-surfaces. The root-mean-square (rms) value describing the surface roughness of the polished sample is 5.12 nm, which declined to 0.72 nm after CMP, signifying that chemical polishing yielded smoother surfaces. However, the leakage current of the chemically polished crystals increased by an order of magnitude. We measured the surface properties using the Hall effect measurement system. The sheet resistivity of polished sample was 1.72×10^{11} ohm/square, which remained stable over the 3 days, but then decreased about one order of magnitude immediately after chemical polishing, to then recover on day 3; this was because the bromine solution yielded a Te-rich surface that has

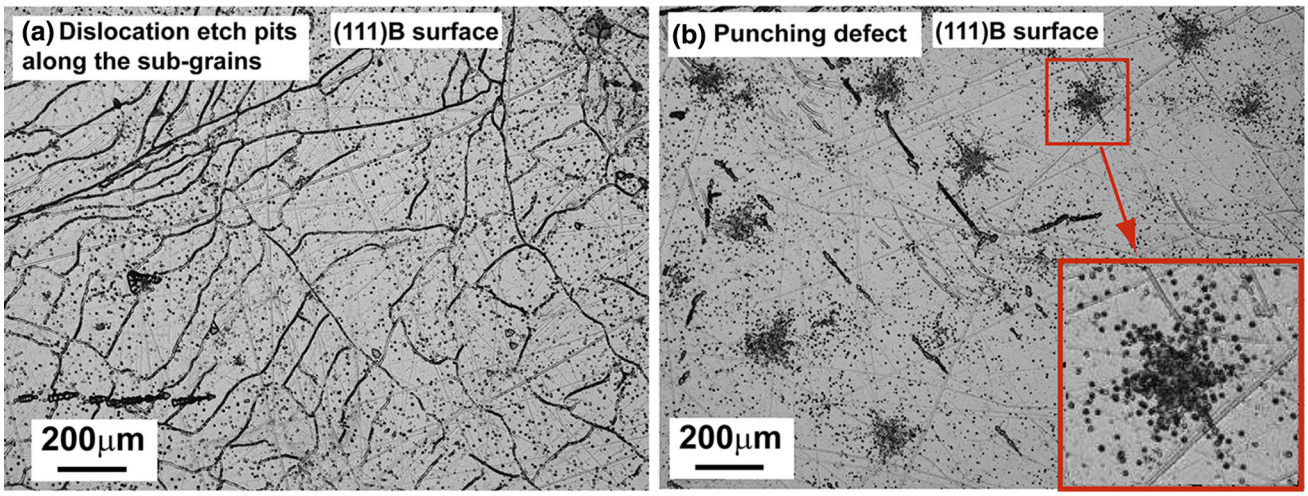

Fig. 1. Optical images of the (111)B surfaces of two CZT crystals etched by a selective etchant. The faint lines in the background are mostly surface scratches. (a) Dislocation etch-pits are evident on the surface, mostly along the sub-grain boundaries. (b) The star-shaped punching defects are revealed on the crystals' surfaces. Such features are usually generated by the interaction of Cd atoms with the Te inclusions during annealing in a Cd overpressure at temperatures above the melting point of Te.

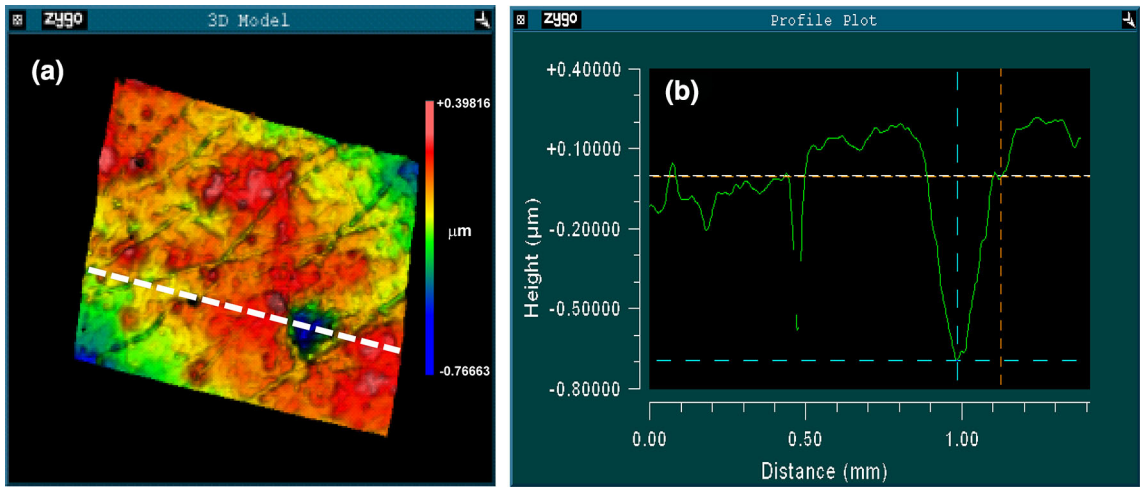

Fig. 2. The surface image and the line profile of an etched CZT surface was taken by an optical profilometer. (a) A 3D image of etched surface. Linear dislocation etch-pits and large punching defects are evident on the surface. (b) A line profile across the defects on the crystal's surface. The large punching defect visible on the surface image has an empty core.

higher conductivity. These surfaces have high affinity to oxidize in air to form a native oxide, and they typically have an increase in the leakage current due to presence of elemental Te.

The XPS peaks in Fig. 4 display evidence of surface oxidation. The Te3d doublet corresponds to the Te elemental state, as apparent from peaks at the binding energies of approximately 572 eV and 583 eV, while two extra peaks appearing at approximately 576 eV and 587 eV reflect the production of the TeO_2 state. The fraction of the chemical shift of the Te3d peaks depended on the exposure time in air after chemical treatment. The doublet of Cd3d was found at approximately 407 eV and 412 eV, corresponding to the elemental peaks of Cd.

This oxidation process usually occurs randomly at the top layer in which the unconverted Te-rich region trapped under it resulted in enhanced leakage current. Passivation is an alternative process to nullify the electrically active Te-rich surfaces more uniformly and permanently. The sheet's carrier concentration, however, is increased by 1–2 orders of magnitude after chemical treatment, most likely due to the formation of more conductive compound(s) after the treatment.

Metal–Semiconductor Interface

The metal–semiconductor interface is an important area to study, wherein the chemical species

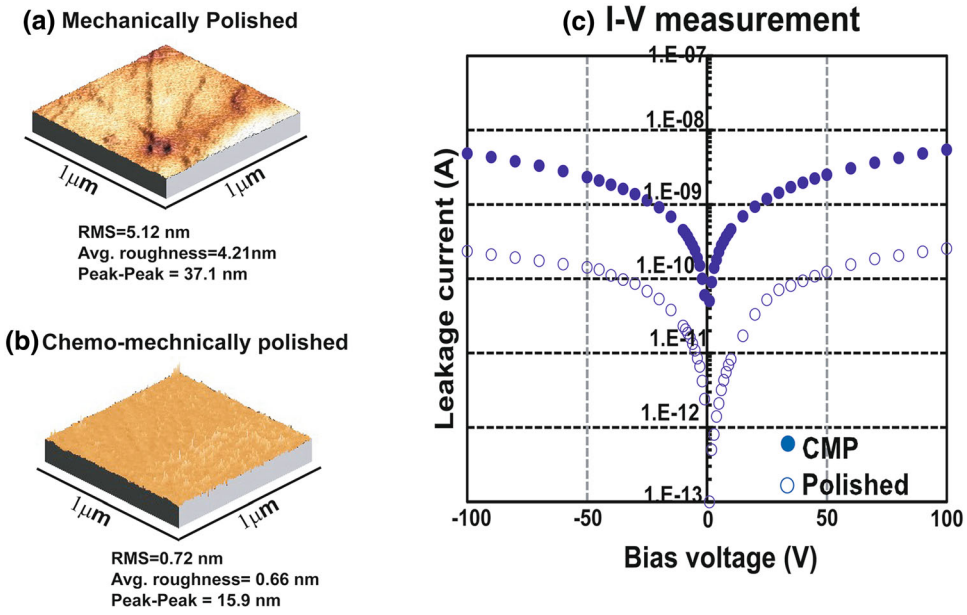

(d) Table -I

CZT Samples	Sheet resistivity Ohm/□		Sheet carrier concentration (1/m²)	
	Day 1	Day 3	Day 1	Day 3
Polished	1.72×10^{11}	1.29×10^{11}	6.71×10^{8}	7.23×10^{8}
CMP	1.00×10^{10}	9.14×10^{10}	3.89×10^{9}	1.64×10^{10}

Fig. 3. (a, b) AFM images of CZT crystal's surfaces before and after chemical polishing. (c) Current–voltage measurement of the corresponding surfaces. Leakage current increased immediately after chemical processing. (d) Data table on the surface resistivity and carrier concentration of polished and CMP-treated surfaces.

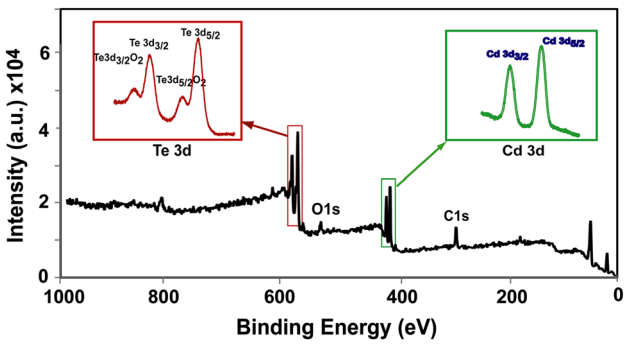

Fig. 4. The spectra from XPS measurements of a chemically treated CZT crystal. The Tellurium 3d doublet had partially shifted to a higher binding energy after forming a stable TeO_2, but the Cd 3d doublet remained the same.

formed during device fabrication create undesirable conditions, and influence the device's performance. We deposited about a 2000-Å-thick layer of Au on a processed CZT surface and investigated the diffusion profile of Au at the Au-CZT interface by the SEM and XPS systems.

As shown in Fig. 5a, the image of the Au-CZT interface, captured by SEM, appeared smooth as desired for fabricating the device. Such a level of surface smoothness was assured by our improved surface-processing technique, which yields a nanoscale surface finish. We also analyzed the diffusion profile of the contact metals that were deposited on the chemically treated surfaces. Figure 5b displays the spectral response of an EDS scan of deposited Au at the three marked areas (1, 2 and 3) at the interface and the near-surface region of the CZT bulk. The EDS result clearly depicts the existence of Au in the CZT bulk but the resolution of the EDS measurement is not enough to determine the diffusion depth. Therefore, we conducted an experiment at XPS on diffusion profile of Au into CZT by gradual material ablation via argon ion sputtering. Once Au is deposited on the CZT surface, the Au-CZT interface layer may extend towards both the surface and bulk, depending on

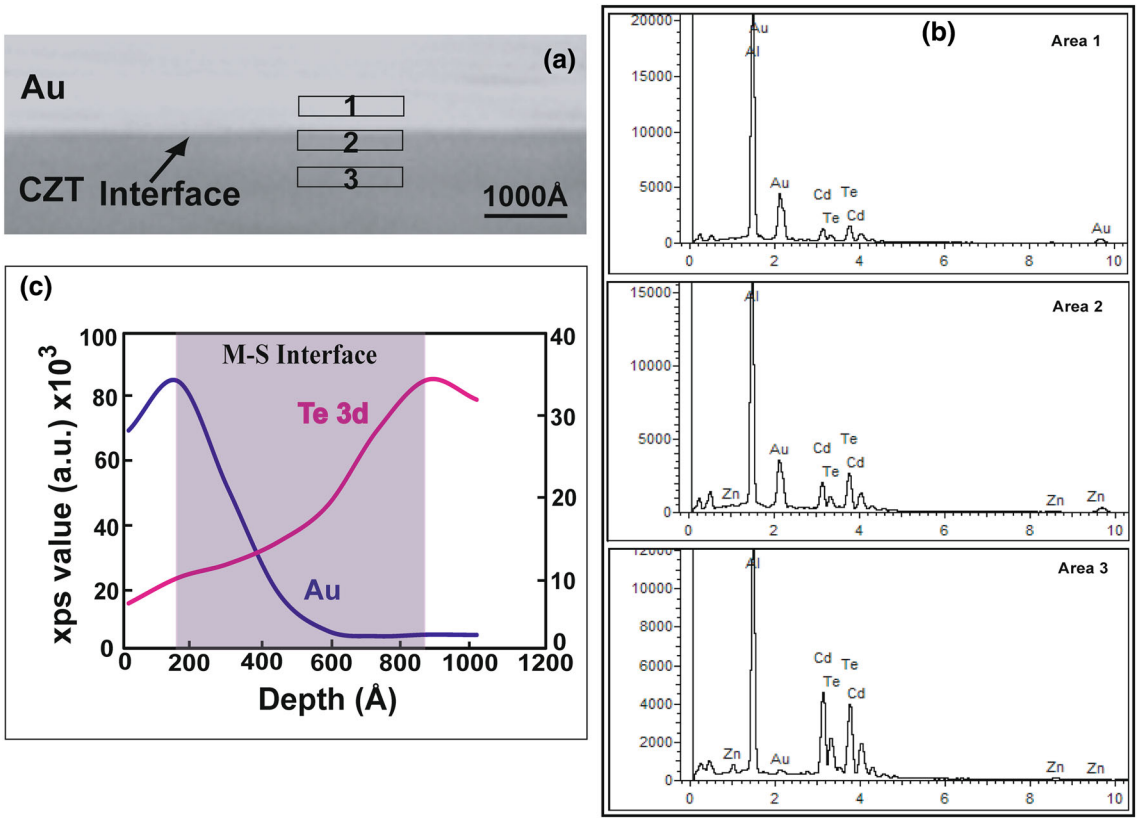

Fig. 5. (a) SEM image of the Au-CZT interface. Marks *1*, *2* and *3* are the EDS scan areas. (b) EDS peaks measured at the marked area around the interface. The peaks indicate the diffusion of Au into the CZT bulk. (c) Au diffusion profile at the interface extracted from the XPS measurements.

the deposition method, metal and condition. Figure 5c shows the diffusion profile of deposited Au on the CZT surface. It seems that Au diffused into the CZT to a depth of approximately 600 Å. These results are consistent with the EDS data.

CONCLUSIONS

Our experimental data demonstrated the presence of sub-grains and dislocations in most of the commercial CZT crystals, and star-shaped punching defects in only annealed crystals. The sub-grains and dislocations are usually extended towards various crystallographic orientations and emerged on the surface of the crystals, while the punching defects are randomly distributed throughout the crystals. These extended defects likely influence epilayer materials grown on it, and the performance of fabricated x-ray, gamma and infrared devices. Our surface-processing technique yielded sub-nano-scale (rms value 0.72 nm) surface smoothness with sheet resistivity in the range of 10^{10}–10^{11} ohm/square, and improved the carrier concentration by up to two orders of magnitude. Furthermore, the degree of surface smoothness produced a microscopic flat and smooth interface, which helped to enhance the carrier transportation as well.

REFERENCES

1. R.B. James, T.E. Schlesinger, J.C. Lund, and M. Schieber, *Semiconductors for Room Temperature Nuclear Detector Applications*, vol. 43, ed. R.B. James and T.E. Schlesinger (New York: Academic, 1995).
2. C. Szeles, *IEEE Trans. Nucl. Sci.* NS-51, 1242 (2004).
3. J. Garland and R. Sporken, *Mercury Cadmium Telluride Growth, Properties and Applications*, ed. P. Capper and J. Garland (Wiley, Chichester, 2011).
4. R. Singh, S. Velicu, and J. Crocco, et al., *J. Electron. Mater.* 34, 885 (2005).
5. T.E. Schlesinger, J.E. Toney, H. Yoon, E.Y. Lee, B.A. Brunett, L. Franks, and R.B. James, *Mater. Sci. Eng.* R32, 103 (2001).
6. C. Szeles, S.E. Cameron, J.-O. Ndap, and W.C. Chalmers, *IEEE Trans. Nucl. Sci.* NS-49, 2535 (2002).
7. A.E. Bolotnikov, N.M. Abdul-Jabbar, O.S. Babalola, G.S. Camarda, Y. Cui, A.M. Hossain, E.M. Jackson, H.C. Jackson, J.A. James, K.T. Kohman, A.L. Luryi, and R.B. James, *IEEE Trans Nucl. Sci.* 55, 2757 (2008).
8. A. Hossain, A.E. Bolotnikov, G.C. Camarda, Y. Cui, G. Yang, K.H. Kim, R. Gul, L. Xu, and R.B. James, *J. Cryst. Growth* 312, 1795 (2010).
9. A. Hossain, A.E. Bolotnikov, G.S. Camarda, Y. Cui, D. Jones, J. Hall, K.H. Kim, J. Mwathi, X. Tong, G. Yang, and R.B. James, *J. Electron. Mater.* 43, 2771 (2014).